IBRO Neuroscience Reports 15 (2023) 179–185

Contents lists available at ScienceDirect

IBRO Neuroscience Reports

journal homepage: www.sciencedirect.com/journal/IBRO-Neuroscience-Reports

Research paper

Measurement of thalamus and cortical damages in hypoxic ischemic encephalopathy

GyeongMo Sohn [1], Sung Eun Kim [2,*]

Department of Neurology, Haeundae Paik Hospital, Inje University College of Medicine, Busan, Republic of Korea

ARTICLE INFO

Keywords:
Hypoxic-ischemic encephalopathy
Prognostication
Thalamic gray-white matter ratios
Suppression ratios
Thalamocortical circuit

ABSTRACT

Background: The thalamic gray-white matter ratios (GWRs) on CT and quantitative suppression ratios (SRs) of background activities on EEG may reflect damages in the thalamus and cerebral hemispheres in patients with hypoxic-ischemic encephalopathy (HIE).

Methods: The inclusion criteria were (1) cardiac arrest patients over the age of 20 years from March 2010 to March 2020, and (2) patients who had both EEG and brain CT within 7 days after cardiac arrest. The thalamic GWRs were semi-quantitatively measured by using the region of interest (ROI). SRs of background were analyzed with the installed software (Persyst® v13) in EEG machine.

Results: 175 patients were included among 686 patients with HIE and the thalamic GWRs of 168 patients were successfully measured. 155 patients (89 %) showed poor outcomes. The poor outcome group revealed not only higher SRs, but also lower thalamic GWRs. The thalamic GWRs showed a negative correlation to the SRs (ρ (rho) $= -0.36$, $p < 0.0001$ for right side, ρ (rho) $= -0.31$, $p < 0.0001$ for left side). The good outcome group showed neither beyond the cut-off values of thalamic GWRs nor SRs [40 % (59/148) VS 0 % (0/20) in right side, $p = 0.0005$ %, and 28 % (42/148) VS 0 % (0/20) in left side, $p = 0.0061$].

Conclusion: The thalamic GWRs and SRs may reflect the damage in the thalamus and cerebral hemispheres in patients with HIE. Insults in the thalamocortical circuit (TCC) or the thalamus might be responsible for the poor outcome.

1. Introduction

Hypoxic-ischemic encephalopathy (HIE) after a cardiac arrest has been known to cause a severe brain damage. The thalamus and cerebral cortices are known to be the most vulnerable parts of the brain after a hypoxic injury (Gofton et al., 2009;Sandroni et al., 2021). The thalamocortical circuit (TCC) is important for a maintenance of consciousness, and it is known to play a critical role in the recovery from a severe brain damage (Ahissar and Oram, 2015;Shepherd and Yamawaki, 2021). Unfortunately, a complete recovery from HIE can possibly be expected in only a few patients who achieved the return of spontaneous circulation from a cardiac arrest (Nolan et al., 2021). If the damages in the thalamus and cerebral cortices can be measured somehow, we may utilize it for a prognostication.

CT is a very useful diagnostic tool to evaluate anatomical structures especially in an emergent situation. The Hounsfield unit (HU) is a relatively quantitative measurement of radio density on CT. Every tissue on CT has its unique HU, so that measuring the ratio of HU between the gray and white matter could reflect the status of brain damages in patients with HIE (Lopez Soto et al., 2020). Moreover, measuring the gray-white matter ratio (GWR) of HU on CT is a simple and reliable method (Sohn et al., 2022). Previous studies have reported that the GWRs in specific structures successfully predicted a poor outcome in patients with HIE (Lee et al., 2013;Wu et al., 2011).

Moreover, background activities on EEG have been used as a prognostic tool in patients with HIE (Admiraal et al., 2019;Hofmeijer et al., 2015;Hofmeijer and van Putten, 2016;Ruijter et al., 2019;Sondag et al., 2017). Even though malignant EEG patterns such as suppression, burst-suppression with or without periodic discharges have been regarded as a poor prognostic factor in patients with HIE (Westhall et al.,

* Correspondence to: Department of Neurology, Haeundae Paik Hospital, Inje University College of Medicine, Haeundae-ro 875, Haeundae-gu, Busan 48108, Republic of Korea.
E-mail address: epidoc@inje.ac.kr (S.E. Kim).
[1] https://orcid.org/0000–0002-9526–6877
[2] https://orcid.org/0000–0002-7099–1749

https://doi.org/10.1016/j.ibneur.2023.09.002
Received 12 March 2023; Received in revised form 4 September 2023; Accepted 4 September 2023
Available online 6 September 2023

2016), recent studies have suggested that a background activity quantification could also be a possible biomarker for prognostication (Amorim et al., 2019;Tjepkema-Cloostermans et al., 2017).

We hypothesized that the thalamic GWRs and quantitative measurement of background activities would possibly reflect the severity of damages in the thalamus and cerebral cortices, therefore, have a role for prognostication in patients with HIE.

2. Methods

2.1. Subjects

This is a retrospective cohort study conducted at single university hospital. The institutional review board approved this study, and waived an informed consent. Inclusion criteria were 1) cardiac arrest patients over 20 years old from March 2010 to March 2020, and 2) patients who were evaluated with both EEG and brain CT within 7 days after cardiac arrest. Some of the patients received the standard care with targeted temperature management (TTM, 34 °C for 48 h).

2.2. Data acquisition

We collected clinical, electrographic, and radiographic data. The clinical data included age, sex, absence/presence of brainstem reflexes, and cerebral performance category (CPC) score at discharge. The good outcome was defined as 1 or 2 of CPC score and the poor outcome was defined as CPC score 3,4, and 5. The clinical evaluation was conducted within 3 days after cardiac arrest.

The thalamic GWRs were semi-quantitatively measured using the region of interest (ROI). The non-enhanced brain CT (B-CT CE-) was reviewed on the archiving system and analyzed using the provided tools (m-view 5.4, Marotech Inc., South Korea). We previously proved the merit of this ROI measurement (Sohn et al.,2022). The size (30 mm^2) and location of ROI were standardized within the splenium of the corpus callosum (CC) and the thalamus. The axial planes that most reliably demonstrated the lateral ventricle, thalamus, and CC were selected. A circular ROI was placed at the target structures on the axial B-CT CE- while avoiding the CSF space. The measurement with ROI was repeated 3 times and the mean value was obtained (Fig. 1). The GWR was calculated using the HU at the thalamus and CC: Thalamic GWR=HU at the thalamus/HU at the CC.

The CT scan was performed using a 128-row CT scanner (Definition AS+, Siemens Healthcare, Forchheim, Germany) with 120 kVp, 350–400 mAs, gantry rotation time = 0.5 s, reconstruction kernel = H31s medium smooth+ , and slice thickness= 5 mm. The matrix size of each slice is 512 mm × 512 mm, displayed FOV is 250 mm × 250 mm, and one pixel size is 0.412 mm × 0.412 mm. Therefore, the ROI contains a total of 73 (30 mm^2/0.412 mm^2) pixels. The thalamic GWRs were also measured in age and sex matched 52 normal controls in order to calculate inter-personal agreement. The definition of abnormal CT findings (increased intra-cranial pressure, IICP) included any signs of IICP such as effacement of the ventricles, basal cisterns and other CSF spaces, or brain herniation or loss of the gray-white matter differentiation (Ohle et al., 2015).

All EEG recordings were performed with 19 electrodes placed on the scalp according to the international 10–20 system. Impedances were maintained below 5 kΩ before starting the recording and measured again at the end of the recording under the following settings: sampling rate = 250 Hz; low filter = 0.5 Hz; and high filter = 70 Hz. Intravenous sedatives (remifentanil (3.5 mcg/kg/h), midazolam (0.05 mg/kg/h), propofol (2.5 mg/kg/h)) should be discontinued 30 min prior to EEG and not be used during EEG recording. The EEG was recorded for at least 30 min. The EEG was performed 3 days after cardiac arrest.

The malignant EEG patterns were defined as suppression /burst-suppression with or without rhythmic and periodic patterns (RPPs) (Westhall et al., 2016). The suppression was defined as voltage activity < 10 μV with > 99 % periods of suppression, and the burst-suppression was defined as voltage activity < 10 μV with 50–99 % periods of suppression. The RPPs were defined as suggestion from the guideline of American Clinical Neurophysiology Society (ACNS) (Hirsch et al., 2021). The quantitative background activities were analyzed with suppression ratio (SR). The SR of background was analyzed with installed software (Persyst® v13) in an EEG machine. Previously, we described the detailed method in another study (Lee et al., 2021). In brief, the SR of the background activities was calculated as an average percentage of background EEG activities below a user-specified amplitude threshold. The parameter settings were as follows: epoch duration = 10 s; flat duration threshold = 0.5 s; flat duration amplitude = 3μV; and running average duration = 60 s. Time-SR plot was generated and the highest value of the SR was obtained in order to analyze the SR (Fig. 2).

2.3. Statistical analysis

The thalamic GWR measurement was evaluated by independent two

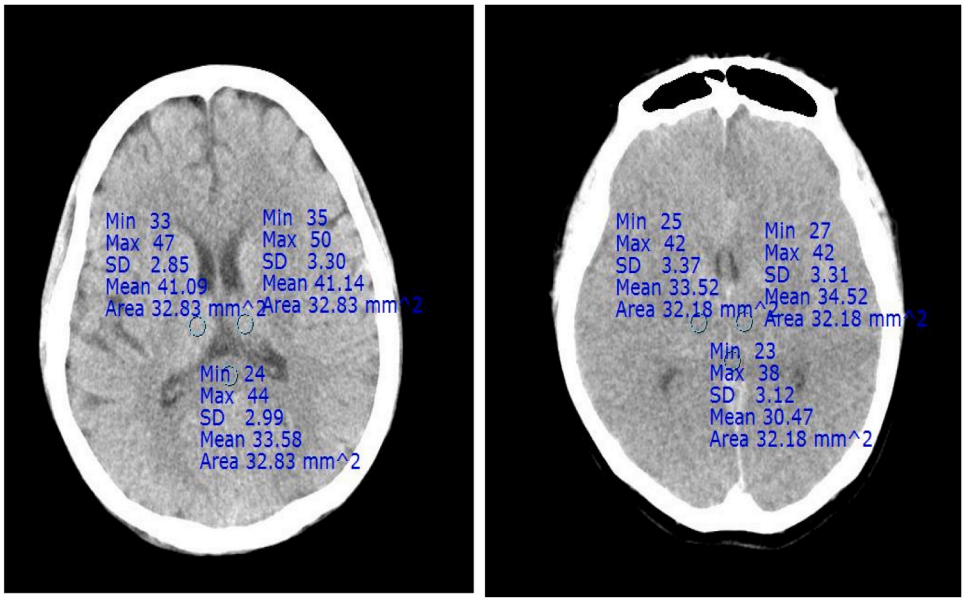

Fig. 1. Application of ROI for the thalamic GWR. The size (30 mm^2) and location of ROI were standardized within the posterior part (splenium) of the CC and thalamus. The axial plans that most reliably demonstrated the lateral ventricle, thalamus and CC were selected. A circular ROI was placed at the target structures on the axial B-CT CE- while avoiding the CSF space. The measurement with ROI was repeated 3 times and the mean value was obtained. The GWR was calculated using HU at the thalamus and CC: Thalamic GWR=HU at the thalamus/HU at the CC. B-CT CE-: brain computed tomography without contrast enhancement, CC: corpus callosum, CSF: cerebrospinal fluid, GWR: gray-white matter ratio, HU: Hounsfield unit, ROI: region of interest.

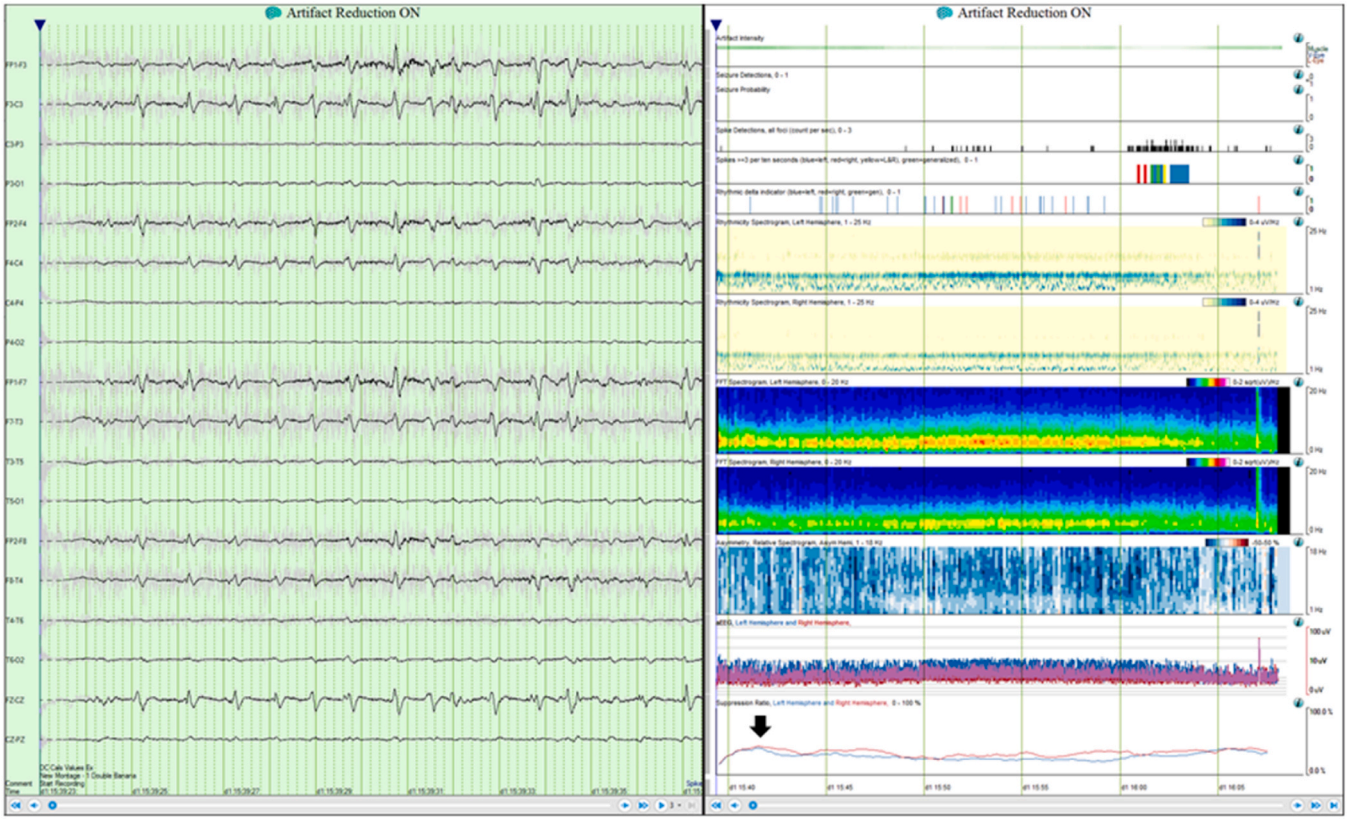

Fig. 2. Quantitation of background suppression ratio. The suppression ratio trend displays a running average (60 s) of percentage of EEG activity that fell below 3μV lasting 0.5 s (the default threshold values in Persyst version 13). The raw data of each suppression ratio is extracted to indicate the highest value observed (arrow).

neuroradiologists who have more than 10 years experiences. The kappa value of interpersonal and intrapersonal agreement was calculated with 52 normal controls and 9 patients. The demographics and clinical characteristics were compared between groups (poor VS good outcomes) using the chi-squared test or Fisher's exact test for categorical variables and Student's t-test or the Mann–Whitney U test for numerical variables. A *p*-value of < 0.05 was considered to indicate statistical significance for all calculations. The receiver operating characteristic analysis (ROC) was applied for calculating area under curve (AUC) for predicting a poor outcome. In our study group, the poor prognosis group (89 %) is much larger than the good prognosis group (11 %); it is a skewed deviation population. Therefore, ROC curve analysis might not be the best option. However, we used a ROC curve for the statistical analysis because it is still well-established systematic tool for quantifying the impact of variability among individuals' decision thresholds. The diagnostic value of each variable for predicting a poor outcome was expressed as sensitivity, specificity, positive predictive value (PPV), and negative predictive value (NPV). In addition, Spearman's rank correlation coefficient was used to correlate between the thalamic GWRs and SRs. All statistical tests were performed using MedCalc® version 19.5.2 (MedCalc Software Ltd, Ostend, Belgium; https://www.medcalc.org; 2020).

3. Results

3.1. Reliability of the thalamic GWRs and clinical demographics

The measurement of the thalamic GWRs was reliable and stable. The kappa value of interpersonal agreement was good (right thalamus= 0.74, left thalamus= 0.79 and CC= 0.79), and intrapersonal agreement was also good (right thalamus = 0.89, left thalamus= 0.89 and CC= 0.83), reflecting dependence of personal anatomical landmark of the target structures.

Of 686 patients with HIE, a total of 175 patients were included. Table 1 shows the clinical characteristics of enrolled 175 patients with HIE. Of 175 patients for this study, the thalamic GWRs were successfully measured in 168 patients, and we failed to measure the thalamic GWRs of the rest 7 patients due to severe distortions of the target structures. Of 175 patients with HIE, 89 % (155/175) showed poor outcomes and 11 % (20/175) showed good outcomes. The percentage of malignant EEG patterns, SRs, and thalamic GWRs were significantly different between groups. The poor outcome group showed higher SRs as well as lower thalamic GWRs compared to the good outcome group. The age was

Table 1
Clinical characteristics.

	Poor prognosis *	Good prognosis	*p*-value
n	155	20	
Age [median (range**, years)]	63 (50–75)	50 (41–62)	0.016
Sex (male: female)	1.4:1 (90:65)	1.9: 1 (13:7)	0.55
With TTM (%)	42 (65/155)	65 (13/20)	0.051
Malignant EEG* ** (%)	84 (130/155)	10 (2/20)	< 0.0001
Gray-white matter ratio, Rt [median, (range**)]	1.23 (1.17–1.29)	1.26 (1.23–1.32)	0.038
Gray-white matter ratio, Lt [median, (range**)]	1.23 (1.17–1.29)	1.27 (1.23–1.32)	0.049
Suppression ratio, Rt [median, (range**), %]	58.5 (9.7–91.6)	7.0 (0.6–13.3)	< 0.0001
Suppression ratio, Lt [median, (range**), %]	64.9 (11.3–95.4)	8.8 (1.0–24.3)	< 0.0001

* poor prognosis=CPC 3–5; **interquartile range; ***malignant EEG=burst-suppression or suppression with or without rhythmic periodic patterns; TTM=targeted temperature management; EEG and brain CT were evaluated within 3 days (interquartile range 2–4 days) and within 3 days (interquartile range 2–5 days), respectively

significantly older in the poor outcome group, but the sex ratio was not different between groups. The median times for performing EEG and CT were as follows; 3 days for EEG (interquartile range 2–4 days) and 3 days for B-CT CE- (interquartile range 2–5 days).

3.2. Correlation between the thalamic GWRs and SRs

The thalamic GWRs were significantly decreased in patients with HIE compared to normal controls. The ROC analysis showed that the cut-off values of the right and left thalamic GWRs for differentiating between HIE and normal control were ≤ 1.27 (AUC in right side= 0.76, $p < 0.001$ and AUC in left side= 0.74, $p < 0.001$). Also, the cut-off values of thalamic GWRs differentiating between a poor and good outcome were ≤ 1.24 in right side (AUC= 0.64, $p = 0.014$) and ≤ 1.20 in left side (AUC= 0.64, $p = 0.017$). Table 2 shows the thalamic GWRs according to the clinical variables, which revealed more decreased values in more severely damaged conditions; the thalamic GWRs were significantly decreased in the poor outcome, death, and abnormal CT finding groups. Furthermore, the thalamic GWRs predicted a poor outcome as same as abnormal CT findings on visual analysis did; the AUCs in abnormal CT findings (AUC= 0.65, $p < 0.001$) were not different from those in the thalamic GWRs [≤ 1.24 in right side (AUC= 0.64, $p = 0.014$) and ≤ 1.20 in left side (AUC= 0.64, $p = 0.017$)].

There was also the same trend in SRs, but the trend of SRs showed opposite direction to that of the thalamic GWRs. Table 2 shows the SRs according to clinical variables, which revealed higher values in more severely damaged conditions; the SRs were significantly higher in groups with a poor outcome, death, and malignant EEG pattern. Furthermore, the SRs predicted a poor outcome as same as the malignant patterns on EEG did (AUC in malignant pattern on EEG=0.87, $p < 0.001$ and AUC in right SR= 0.8, $p < 0.001$, AUC in left SR= 0.78, $p < 0.001$). In addition, the cut-off values of the right (>21.5 %, AUC= 0.8, $p < 0.001$) and left SRs (>42.6 %, AUC= 0.78, $p < 0.001$) successfully predicted a poor outcome.

Table 3 shows the diagnostic accuracy of the thalamic GWRs and SRs for predicting a poor outcome. The specificity and PPV of the thalamic GWRs and SRs were as high as those of the malignant patterns on EEG and IICP signs on CT. Especially, PPVs of the thalamic GWRs and SRs were more than 90 %. However, the sensitivity and the NPV were lower than those of the malignant patterns of EEG.

In addition, the thalamic GWRs showed negative correlation to the SRs (Fig. 3). This correlation may explain synchronous damages of the thalamus and cerebral cortices, which represent the thalamic GWRs and SRs, respectively. Table 4 shows that the damages in either thalamus or cerebral cortices may be responsible for a poor outcome.

Table 2
Thalamic gray-white matter ratios and suppression ratios according to clinical variables.

The thalamic gray-white matter ratio (Median, IQR)		
	Right	Left
Poor VS Good outcome	1.23 (1.17–1.29) VS 1.26 (1.17–1.29)	1.23 (1.17–1.29) VS 1.27 (1.23–1.32)
Death VS Survivor	1.22 (1.14–1.27) VS 1.26 (1.20–1.32)	1.22 (1.17–1.27) VS 1.26 (1.20–1.32)
Abnormal VS Normal CT findings	1.18 (1.12–1.23) VS 1.26 (1.21–1.32)	1.19 (1.12–1.23) VS 1.26 (1.21–1.33)
The suppression ratio (%, Median, IQR)		
	Right	Left
Poor VS Good outcome	58.5 (9.7–91.6) VS 7.0 (0.7–13.3)	64.9 (11.3–95.4) VS 8.8 (1.0–24.3)
Death VS Survivor	82.9 (21.3–96.4) VS 14.4 (3.0–62.1)	86.5 (28.1–96.8) VS 19.1 (4.4–70.3)
Malignant VS Benign patterns on EEG	73.2 (19.1–95.8) VS 5.9 (1.2–13.6)	80.9 (26.2–96.4) VS 6.8 (0.8–18.0)

All of the GWRs and SRs were significantly different between the clinical variables. GWR: gray-white matter ratio, IQR: interquartile range, SR: suppression ratio

Table 3
Predicting values for poor outcome*.

	n	Sensitivity (%)	Specificity (%)	PPV (%)	NPV (%)
Malignant EEG	175	84 (130/155) (77.1–89.3)	90 (18/20) (68.3–98.8)	98 (130/132) (94.6–99.6)	42 (18/43) (32.8–51.5)
Suppression ratio	175				
Right (>21.5)		63 (98/155) (55.1–70.8)	95 (19/20) (75.1–99.9)	99 (98/99) (93.5–99.9)	25 (19/76) (20.9–29.4)
Left (>34.4)		63 (97/155) (54.5–70.2)	85 (17/20) (62.1–96.8)	97 (97/100) (91.9–98.9)	23 (17/75) (18.2–27.8)
Gray-white matter ratio	168				
Right (≤1.24)		54 (80/148) (45.7–62.3)	75 (15/20) (50.9–91.3)	94 (80/85) (88.1–97.2)	18 (15/83) (14.0–23.1)
Left (≤1.20)		36 (54/148) (28.7–44.8)	90 (18/20) (68.3–98.8)	96 (54/56) (87.7–99.0)	16 (18/112) (13.7–18.8)
IICP signs on CT	175	33 (52/155) (26.2–41.6)	100 (20/20) (83.2–100)	100 (52/52) (93.2–100)	16 (20/123) (14.8–17.8)

* poor prognosis=CPC 3–5; malignant EEG=burst-suppression or suppression with or without rhythmic periodic patterns; EEG and brain CT were evaluated within 3 days (interquartile range 2–4 days and 2–5 days, respectively). CPC: cerebral performance category, IICP: increased intracranial pressure, NPV: negative predictive value, PPV: positive predictive value

4. Discussion

This study demonstrated that measuring the thalamic GWRs was a stable and reliable way to evaluate the severity of hypoxic injuries. Intra-person agreement was higher than inter-person agreement. This is probably because the anatomic landmark for measurement could be slightly different between observers. We repeated measurements 3 times in order to decrease the bias of values, and the average value was obtained. Decreased thalamic GWRs were related to poor outcomes, deaths, and IICP signs on CT. The pathophysiology of decreased thalamic GWRs might be related to IICP. IICP with increasing water content in gray matter would decrease the HU at the thalamus, resulting in a lower value of the thalamic GWRs. Other studies also showed that GWRs on B-CT CE- could predict outcomes of patients with HIE (Lee et al., 2013;Lopez Soto et al., 2020;Wu et al., 2011). The thalamus has been regarded as one of the target structures in HIE. There are several studies that have evaluated GWRs of the thalamus as a predictive marker (Kenda et al., 2021;Wu et al., 2011). Other studies have evaluated the basal ganglia GWRs based on gray matters such as the caudate nucleus (CN) or putamen to white matters such as the posterior limb of the internal capsule or CC (Lee et al., 2011). Also, there is electrophysiological study that looked at phenomenon generated by damaged thalami (Endisch et al., 2016). The anatomical landmarks of the CN or putamen are evident in a normal population, although it is not feasible to measure it in patients with HIE due to the distortion of structures. On the other hand, it is relatively easy to measure the thalamus in IICP conditions. We were able to measure the ROI at the thalamus, although the CN or putamen was distorted. The fact that 96 % (168/175) of thalamic GWRs were successfully measured in our study raises a question that measuring the thalamus might be a better choice rather than CN or putamen in HIE patients.

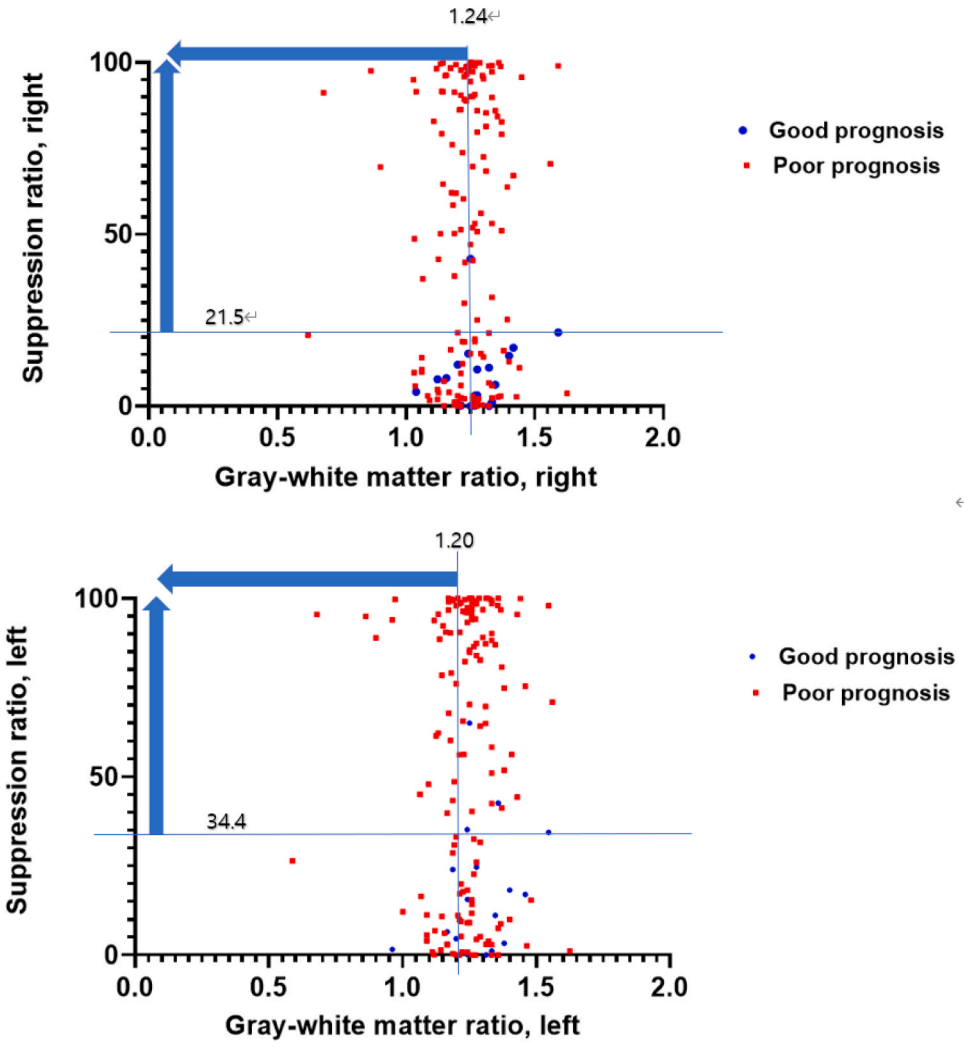

Fig. 3. The correlation between thalamic gray-white matter ratios and suppression ratios. Predicting values for poor outcome were left > 34.4 and right > 21.5 of suppression ratios, left < 1.20 and right < 1.24 of the thalamic gray-white matter ratios. Thalamic gray-white matter ratios were negatively correlated with suppression ratios (Spearman's coefficient of rank correlation $= -0.36$, $p < 0.0001$ for right side, Spearman's coefficient of rank correlation$= -0.31$, $p < 0.0001$ for left side). Good prognosis = CPC score 1–2, Poor prognosis=CPC score 3–5.

Table 4
The thalamic gray-white matter ratios and suppression ratios in the thalamus level, cortex level, and thalamocortical level.

	Poor outcome	Good outcome	*p*-value
Thalamus level			
Right thalamic GWR (≤1.24)	80/148	5/20	0.015
Left thalamic GWR (≤1.20)	54/148	2/20	0.018
Cortex level			
Right suppression ratio (>21.5)	54/148	1/20	< 0.0001
Left suppression ratio (>34.4)	97/155	3/20	0.0001
Thalamocortical level			
Right thalamic GWR-Right suppression ratio	59/148	0/20	0.0005
Right thalamic GWR-Right suppression ratio	42/148	0/20	0.0061

GWR: gray-white matter ratio, Good outcome = CPC 1–2, Poor outcome = CPC 3–5

The IICP signs on CT have been known as a reliable factor to predict a poor outcome (Ohle et al., 2015). Our study showed that AUC of the thalamic GWRs were not as different as that of IICP signs on CT in terms of predicting a poor outcome, suggesting a merit of measurement of the thalamic GWRs as interpretation of IICP signs on CT may vary depending on interpreter's experience level. Plus, the sensitivity of thalamic GWRs was higher than that of IICP signs on CT.

The SR in this study was defined as a degree of suppressed background activity less than 3 μV which is a stricter definition than the ACNS definition of less than 10 μV (Hirsch et al., 2021). The SRs were independent on the modalities of EEG such as rEEG or cEEG, although the SRs could be impacted by sedatives. Therefore, we avoided any sedative medications 30 min prior to performing EEG. The SR is a reliable measurement confirmed in the previous study (Lee et al., 2021). Higher SRs were observed in patients who had severe brain damages and poor outcomes. This study also demonstrated that the SR was not inferior to the malignant EEG patterns in terms of predicting a poor outcome. Although the ACNS has suggested the definition of malignant EEG patterns (Hirsch et al., 2021), the interpretation is still challenging. Therefore, the SR may be a better alternative for evaluating damages in the cerebral cortices.

The malignant EEG patterns are well described for predicting a poor outcome in many literature articles (Hofmeijer et al., 2015;Hofmeijer and van Putten, 2016;Nolan et al.,2021;Ruijter et al., 2019;Sondag et al., 2017;Spalletti et al., 2016;Westhall et al., 2016). However, there were two cases who had malignant EEG patterns among 20 patients of the good prognosis group. One patient was a 27 years old female who attempted a suicide with hanging. Patient had no past medical history except a major depression. Reportedly, patient was brought by her family member and achieved a ROSC within 15 min. Although the event caused a moderate cerebral disability with CPC score 2 after all, she was classified into a good outcome group because we defined good outcome as CPC score from 1 to 2. The other patient was a previously healthy 45 years old male with a medical history of small bowel perforation. He

underwent a surgery, but had a cardiac arrest while in the recovery room. Fortunately, patient achieved a ROSC within 10 min. He also had a moderate cerebral disability with CPC score 2 after all, but he is now ambulatory and able to pursue daily activities without assistance.

The TCC damages in HIE might be related with a poor outcome. Thus, evaluation of TCC function in HIE patients would be important. There are known prognostication methods such as clinical, electrophysiological, or serological markers in HIE patients (Nolan et al., 2021). Only a few studies have focused on the function of TCC, showing the different patterns of connectivity at default mode network, thalamic or hippocampal network in patients with a poor outcome. It suggests a predictive value of resting state fMRI or LORETA with EEG in HIE (De Stefano et al., 2020;Pugin et al., 2020;Wagner et al., 2020). Although nothing has been suggested as a gold standard for evaluating the function of TCC in HIE, the thalamic GWRs and SRs might be utilized for gauging the degree of TCC damages. Our study demonstrated that the good outcome group showed neither beyond the cut-off values of thalamic GWRs nor SRs. The thalamic GWRs and SRs were not measured simultaneously in our study, but the time of independent acquisition was not different; 3 days for EEG (interquartile range 2–4 days) and 3 days for B-CT CE- (interquartile range 2–5 days). We believe the thalamic GWRs and SRs may reflect the severity of TCC damages in HIE.

This study has several limitations. First, as we only analyzed selected patients who had both B-CT CE- and EEG, there may be a selection bias. The cohort in our study involved only 10% good outcome patients, which is less than the usual 30 % reported in large registry or cohort out-of-hospital cardiac arrest (OHCA) (Wang et al., 2020). This may have been due to the selection bias. Withdrawing life-sustaining therapy due to perceived poor neurological prognosis (WLST-N) is a common cause of hospital death after OHCA (Elmer et al., 2016). Because the results of GWRs and SRs were not used to decide on WLST-N in our study, likelihood of incorporation bias would be very low.

Second, the outcome was evaluated with CPC at discharge, which is not always reflecting the consequences of HIE. The mortality could be resulted from other underlying medical conditions such as sepsis. We need a prospective study aiming for a long-term outcome.

Third, measurement of the thalamic GWRs could be insufficient because the ROI (30 mm^2) was not large enough to cover the entire thalamus. In order to diminish variations of the thalamic GWRs, we measured 3 times for obtaining an average value. In addition, there were good interpersonal and intrapersonal agreements.

Finally, the thalamic GWRs and SRs were not simultaneously measured. We believe the following study evaluating the TCC simultaneously by using such as resting state fMRI or fMRI-EEG would be necessary.

Ethical Approval

This study is a retrospective study with the IRB approval number (2020–03–022) and use of informed consent was waived.

CRediT authorship contribution statement

G.M. Sohn contributed in drafting of the work and ensuring that questions related to the accuracy or integrity of the work are appropriately investigated and resolved. S.E. Kim contributed in conceptualization of the work and revising it critically for important intellectual content.

Declaration of Competing Interest

Authors have no known competing financial interests or personal relationships that could have appeared to influence the work reported in this paper.

Acknowledgment

Thanks to GraphPad Prism 9 for us to demonstrate the Fig. 3.

References

Admiraal, M.M., van Rootselaar, A.F., Hofmeijer, J., Hoedemaekers, C.W.E., van Kaam, C.R., Keijzer, H.M., van Putten, M., Schultz, M.J., et al., 2019. Electroencephalographic reactivity as predictor of neurological outcome in postanoxic coma: a multicenter prospective cohort study. Ann. Neurol. 86, 17–27.

Ahissar, E., Oram, T., 2015. Thalamic relay or cortico-thalamic processing? Old question, new answers. Cereb. Cortex 25, 845–848.

Amorim, E., van der Stoel, M., Nagaraj, S.B., Ghassemi, M.M., Jing, J., O'Reilly, U.M., Scirica, B.M., Lee, J.W., et al., 2019. Quantitative EEG reactivity and machine learning for prognostication in hypoxic-ischemic brain injury. Clin. Neurophysiol. 130, 1908–1916.

De Stefano, P., Carboni, M., Pugin, D., Seeck, M., Vulliémoz, S., 2020. Brain networks involved in generalized periodic discharges (GPD) in post-anoxic-ischemic encephalopathy. Resuscitation 155, 143–151.

Elmer, J., Torres, C., Aufderheide, T.P., Austin, M.A., Callaway, C.W., Golan, E., Herren, H., Jasti, J., et al., 2016. Association of early withdrawal of life-sustaining therapy for perceived neurological prognosis with mortality after cardiac arrest. Resuscitation 102, 127–135.

Endisch, C., Waterstraat, G., Storm, C., Ploner, C.J., Curio, G., Leithner, C., 2016. Cortical somatosensory evoked high-frequency (600Hz) oscillations predict absence of severe hypoxic encephalopathy after resuscitation. Clin. Neurophysiol. 127, 2561–2569.

Gofton, T.E., Chouinard, P.A., Young, G.B., Bihari, F., Nicolle, M.W., Lee, D.H., Sharpe, M.D., Yen, Y.F., et al., 2009. Functional MRI study of the primary somatosensory cortex in comatose survivors of cardiac arrest. Exp. Neurol. 217, 320–327.

Hirsch, L.J., Fong, M.W.K., Leitinger, M., LaRoche, S.M., Beniczky, S., Abend, N.S., Lee, J.W., Wusthoff, C.J., et al., 2021. American clinical neurophysiology society's standardized critical care EEG terminology: 2021 version. J. Clin. Neurophysiol. 38, 1–29.

Hofmeijer, J., van Putten, M.J., 2016. EEG in postanoxic coma: prognostic and diagnostic value. Clin. Neurophysiol. 127, 2047–2055.

Hofmeijer, J., Beernink, T.M., Bosch, F.H., Beishuizen, A., Tjepkema-Cloostermans, M.C., van Putten, M.J., 2015. Early EEG contributes to multimodal outcome prediction of postanoxic coma. Neurology 85, 137–143.

Kenda, M., Scheel, M., Kemmling, A., Aalberts, N., Guettler, C., Streitberger, K.J., Storm, C., Ploner, C.J., et al., 2021. Automated assessment of brain CT after cardiac arrest – an observational derivation/validation cohort study. Crit. Care Med. 49, e1212–e1222.

Lee, B.K., Jeung, K.W., Lee, H.Y., Jung, Y.H., Lee, D.H., 2013. Combining brain computed tomography and serum neuron specific enolase improves the prognostic performance compared to either alone in comatose cardiac arrest survivors treated with therapeutic hypothermia. Resuscitation 84, 1387–1392.

Lee, D.A., Park, K.M., Kim, H.C., Khoo, C.S., Lee, B.I., Kim, S.E., 2021. Spectrum of Ictal-interictal continuum: the significance of 2HELPS2B score and background suppression. J. Clin. Neurophysiol.

Lopez Soto, C., Dragoi, L., Heyn, C.C., Kramer, A., Pinto, R., Adhikari, N.K.J., Scales, D. C., 2020. Imaging for neuroprognostication after cardiac arrest: systematic review and meta-analysis. Neurocrit. Care 32, 206–216.

Nolan, J.P., Sandroni, C., Böttiger, B.W., Cariou, A., Cronberg, T., Friberg, H., Genbrugge, C., Haywood, K., et al., 2021. European resuscitation council and European society of intensive care medicine guidelines 2021: post-resuscitation care. Intensive Care Med. 47, 369–421.

Ohle, R., McIsaac, S.M., Woo, M.Y., Perry, J.J., 2015. Sonography of the optic nerve sheath diameter for detection of raised intracranial pressure compared to computed tomography: a systematic review and meta-analysis. J. Ultrasound Med. 34, 1285–1294.

Pugin, D., Hofmeister, J., Gasche, Y., Vulliemoz, S., Lövblad, K.O., Ville, D.V., Haller, S., 2020. Resting-state brain activity for early prediction outcome in postanoxic patients in a coma with indeterminate clinical prognosis. AJNR Am. J. Neuroradiol. 41, 1022–1030.

Ruijter, B.J., Tjepkema-Cloostermans, M.C., Tromp, S.C., van den Bergh, W.M., Foudraine, N.A., Kornips, F.H.M., Drost, G., Scholten, E., et al., 2019. Early electroencephalography for outcome prediction of postanoxic coma: a prospective cohort study. Ann. Neurol. 86, 203–214.

Sandroni, C., Cronberg, T., Sekhon, M., 2021. Brain injury after cardiac arrest: pathophysiology, treatment, and prognosis. Intensive Care Med. 47, 1393–1414.

Shepherd, G.M.G., Yamawaki, N., 2021. Untangling the cortico-thalamo-cortical loop: cellular pieces of a knotty circuit puzzle. Nat. Rev. Neurosci. 22, 389–406.

Sohn, G., Bae, M.J., Park, J., Kim, S.E., 2022. Semi-quantitative analysis of periventricular gray-white matter ratio on CT in patients with idiopathic normal pressure hydrocephalus. J. Clin. Neurosci. 101, 16–20.

Sondag, L., Ruijter, B.J., Tjepkema-Cloostermans, M.C., Beishuizen, A., Bosch, F.H., van Til, J.A., van Putten, M., Hofmeijer, J., 2017. Early EEG for outcome prediction of postanoxic coma: prospective cohort study with cost-minimization analysis. Crit. Care 21, 111.

Spalletti, M., Carrai, R., Scarpino, M., Cossu, C., Ammannati, A., Ciapetti, M., Tadini Buoninsegni, L., Peris, A., et al., 2016. Single electroencephalographic patterns as specific and time-dependent indicators of good and poor outcome after cardiac arrest. Clin. Neurophysiol. 127, 2610–2617.

Tjepkema-Cloostermans, M.C., Hofmeijer, J., Beishuizen, A., Hom, H.W., Blans, M.J., Bosch, F.H., van Putten, M., 2017. Cerebral recovery index: reliable help for prediction of neurologic outcome after cardiac arrest. Crit. Care Med. 45, e789–e797.

Wagner, F., Hänggi, M., Weck, A., Pastore-Wapp, M., Wiest, R., Kiefer, C., 2020. Outcome prediction with resting-state functional connectivity after cardiac arrest. Sci. Rep. 10, 11695.

Wang, L., Gan, X., Wang, X., Wang, K., Yan, H., Wang, Z., Chen, L., 2020. Does time of day influences outcome in out-of-hospital cardiac arrest patients?: a meta-analysis of cohort studies. Medicine 99, e22290.

Westhall, E., Rossetti, A.O., van Rootselaar, A.F., Wesenberg Kjaer, T., Horn, J., Ullén, S., Friberg, H., Nielsen, N., et al., 2016. Standardized EEG interpretation accurately predicts prognosis after cardiac arrest. Neurology 86, 1482–1490.

Wu, O., Batista, L.M., Lima, F.O., Vangel, M.G., Furie, K.L., Greer, D.M., 2011. Predicting clinical outcome in comatose cardiac arrest patients using early noncontrast computed tomography. Stroke 42, 985–992.